Spin-dependent transport through $Cd_{1-x}Mn_xTe$ diluted magnetic semiconductor quantum dots

Shu-Shen Li, Kai Chang, and Jian-Bai Xia
State Key Laboratory for Superlattices and Microstructures, Institute of Semiconductors, Chinese Academy of Sciences, P.O. Box 912, Beijing 100083, People's Republic of China

Kenji Hirose
Fundamental Research Laboratories, NEC Corporation, 34 Miyukigaoka, Tsukuba 305-8501, Japan
(Received 8 July 2003; published 8 December 2003)

We theoretically investigate the spin-dependent transport through $Cd_{1-x}Mn_xTe$ diluted magnetic semiconductor (DMS) quantum dots (QD's) under the influence of both the external electric field and magnetic field using the recursion method. Our results show that (1) it can get a 100% polarized electric current by using suitable structure parameters; (2) for a fixed $Cd_{1-x}Mn_xTe$ DMS QD, the wider the system is, the more quickly the transmission coefficient increases; (3) for a fixed system length, the transmission peaks of the spin-up electrons move to lower Fermi energy with increasing $Cd_{1-x}Mn_xTe$ DMS QD radius, while the transmission of the spin-down electrons is almost unchanged; (4) the spin-polarized effect is slightly increased for larger magnetic fields; (5) the external static electric field moves the transmission peaks to higher or lower Fermi energy depending on the direction of the applied field; and (6) the spin-polarized effect decreases as the band offset increases. Our calculated results may be useful for the application of $Cd_{1-x}Mn_xTe$ DMS QD's to the spin-dependent microelectronic and optoelectronic devices.

DOI: 10.1103/PhysRevB.68.245306 PACS number(s): 73.61.Ey, 73.21.−b

I. INTRODUCTION

In recent years, much interest has been paid to spintronics (spin transport electronics or spin-based electronics), where it is not the electron charge but the electron spin that carries information, and this offers opportunities for a new generation of devices combining the standard microelectronics with spin-dependent effects that arise from the interaction between the spin of the carrier and the magnetic properties of the material.[1]

Guo[2] investigated the spin-polarized transport through semimagnetic semiconductor heterostructures under the influence of both an external electric field and a magnetic field. The structurally symmetric and asymmetric effects as well as the electric-field effect were stressed. The results indicated that (1) transmission resonances are drastically suppressed for spin electrons tunneling through the symmetric heterostructure under an applied bias; and (2) transmission resonances can be enhanced to optimal resonances for spin-up electrons tunneling through the asymmetric structure with double paramagnetic layers under a certain positive bias, while for spin-down ones tunneling through the same structure, resonances can also be enhanced to optimal resonances but under a certain negative bias. Transmission suppression and enhancement could originate from the magnetic- and electric-field-induced and structure-tuned potentials. Spin-dependent resonant enhancement and negative differential resistances could be clearly seen in the current density. The results in Ref. 2 might shed light on design and applications of spintronic devices.

With the rapid progress in semiconductor growth techniques, it is now possible to fabricate various zero-dimensional diluted magnetic semiconductor (DMS) quantum dot (QD) structures. The novel properties of DMS arise from the strong *sp-d* exchange interaction between the carriers and the magnetic ions Mn^{2+} in DMS structures.[3]

Of particular interest in the spin transport theory for semiconductor systems has been the question whether the quasi-independent electron model can adequately account for the experimental results, or whether many-body, or correlated-electron processes are important. Flatte *et al.* have examined extensively this issue in the diffusive transport regime and have concluded that an independent electron approach alone is quite capable of explaining the measurement results, particularly the room-temperature measurements.[1]

The purpose of the present paper is to establish the calculation method for the single-electron transport through three-dimensional nanostructures of DMS based on the one-dimensional numerical method of Lambin and Vigneron.[4] Then, we will study the single-electron transport through $Cd_{1-x}Mn_xTe/Cd_{1-y}Mg_yTe$ DMS QD system using our method. In more detail, we will study the spin-dependent transport under influence of an external electric field and a magnetic field. The results could be useful for the understanding and exploring of future applications of DMS QD, such as the spin-based transistors, quantum computing, etc.

This paper is arranged as follows, in Sec. II, we give a theoretical model to calculate the conductance through nanostructures. In Sec. III, we show the numerical results. Finally, we give the conclusion in Sec. IV.

II. THEORETICAL MODEL

We consider a DMS QD embedded in another semiconductor material. The DMS QD can be a ball, a disk, or of other shapes. An external magnetic field and an electric field are applied to the system along *z* direction. The effective Hamiltonian can be written as follows:

$$H=\frac{(\mathbf{p}+e\mathbf{A})^2}{2m^*}\pm g_e^*\mu_B B-eFz+V_{exch}+V(\mathbf{r}), \tag{1}$$

where m^* and $\mathbf{p}$ are the electron effective mass and the momentum operator, respectively, $\mathbf{r}=(x,y,z)$ is the position vector of the electron, g_e^* is the electron Landé g factor, $\mathbf{F}=(0,0,F)$ is the external electric field, and $\mathbf{A}$ is the vector potential. In the symmetric gauge,

$$\mathbf{A}=\mathbf{B}\times\mathbf{r}/2=(-y,x,0)B/2. \tag{2}$$

$V(\mathbf{r})$ is the confining potential of the electron in the QD:

$$V(\mathbf{r})=\begin{cases}0 & \text{in the QD}\\ E_c & \text{otherwise.}\end{cases} \tag{3}$$

The exchange interaction term V_{exch} describes the sp-d exchange interaction between the electron and the magnetic ion Mn^{2+},

$$V_{exch}=J_{s-d}\langle S_z\rangle\sigma_z, \tag{4}$$

where $J_{s-d}=-N_0\alpha x_{eff}$, $\langle S_z\rangle=S_0B_J[Sg_{Mn}\mu_B B/k_B(T+T_0)]$, and $S=5/2$ corresponds to the spins of the localized $3d^5$ electrons of the Mn^{2+} ions. $B_J(x)$ is the Brillouin function, N_0 is the number of cations per unit volume; the phenomenological parameters x_{eff} (reduced effective concentration of Mn) and T_0 account for the reduced single-ion contribution due to the antiferromagnetic Mn-Mn coupling, k_B is the Boltzmann constant, μ_B is the Bohr magneton, $g_{Mn}=2$ is the g factor of the Mn^{2+} ion, and $\sigma_z=\pm 1/2$ is the electron spin.

We calculate the transmission by employing the Landauer formula.[5] It is first needed to calculate the effective potential function $V_{eff}(z)$ along the z direction. In the x and y directions, we consider a two-dimensional supercell structure. A unit of the supercell is taken to be large enough so that the transmission through the supercell can be regarded as that in the nonperiodic potential. According to the Bloch theorem, electron states are written in terms of the discrete reciprocal-lattice vectors (k_x+nK_x, k_y+mK_y).[5] k_x and k_y are the wave vectors of the electron in the x and y directions, respectively. The transverse wave functions can be written in the following form

$$\Psi(x,y)=\frac{1}{\sqrt{L_xL_y}}\sum_{n,m}C_{nm}(z)e^{i[(k_x+nK_x)x+(k_y+mK_y)y]}, \tag{5}$$

with $K_x=2\pi/L_x$, $K_y=2\pi/L_y$. L_x and L_y are the normalized lengths along the x and y directions, respectively, and $n,m=0,\ \pm1,\ \pm2,\ldots.$

The matrix elements of the effective Hamiltonian Eq. (1) in the x and y directions can be written as

$$\begin{aligned}H_{nn',mm'}={}&\delta_{nn'}\delta_{mm'}\left\{\frac{\hbar^2}{2m_{xy}^*}[(k_x+nK_x)^2+(k_y+mK_y)^2]\right.\\&\left.\pm g_e^*\mu_B B-eFz+V_{exch}\right\}+(1-\delta_{nn'})\delta_{mm'}\\&\times(-1)^{n-n'}\left[\frac{\omega_c^2L^2}{8\pi^2(n-n')^2}-i\frac{\hbar\omega_c(k_y+mK)}{2(n-n')K}\right]\\&+(1-\delta_{mm'})\delta_{nn'}(-1)^{m-m'}\left[\frac{\omega_c^2L^2}{8\pi^2(m-m')^2}\right.\\&\left.+i\frac{\hbar\omega_c(k_x+nK)}{2(m-m')K}\right]\\&+\frac{1}{L_xL_y}\int V(\mathbf{r})e^{i[(n-n')xK_x+(m-m')yK_y]}dxdy,\end{aligned} \tag{6}$$

where $\omega_c=eB/m^*$ is the electron-cyclotron frequency.

Thus, the effective potential function $V_{eff}^i(z)$ can be derived from Eq. (6) by employing the diagonalization matrix, where the superscript i is the index of the transverse quantized energy. The Schrödinger equation is now changed to the one-dimensional form

$$\frac{P_z^2}{2m_z^*}\Psi(z)+V_{eff}^i(z)\Psi(z)=E\Psi(z). \tag{7}$$

Using the Numerov method,[6] Eq. (7) can be transformed into the three-term differential equation with mesh size h_z,

$$a(z_p)\Psi(z_{p+1})-b(z_p)\Psi(z_p)+c(z_p)\Psi(z_{p-1})=0, \tag{8}$$

where

$$a(z_p)=1-\frac{1}{12}\frac{2m_z^*h_z^2}{\hbar^2}[V_{eff}^i(z_{p+1})-E], \tag{9}$$

$$b(z_p)=2+\frac{5}{6}\frac{2m_z^*h_z^2}{\hbar^2}[V_{eff}^i(z_p)-E], \tag{10}$$

$$c(z_p)=a(z_{p-2}). \tag{11}$$

The discretized equation can be changed into the form

$$S(z_{p-1})=\frac{c(z_p)}{b(z_p)-a(z_p)S(z_p)}, \tag{12}$$

where

$$S(z_p)=\frac{\Psi(z_{P+1})}{\Psi(z_p)}. \tag{13}$$

Using the boundary condition for the entrance and the exit, we can calculate the wave function in the entrance, $\Psi(z_0)$. The transmission amplitude for the index in the exit is calculated as

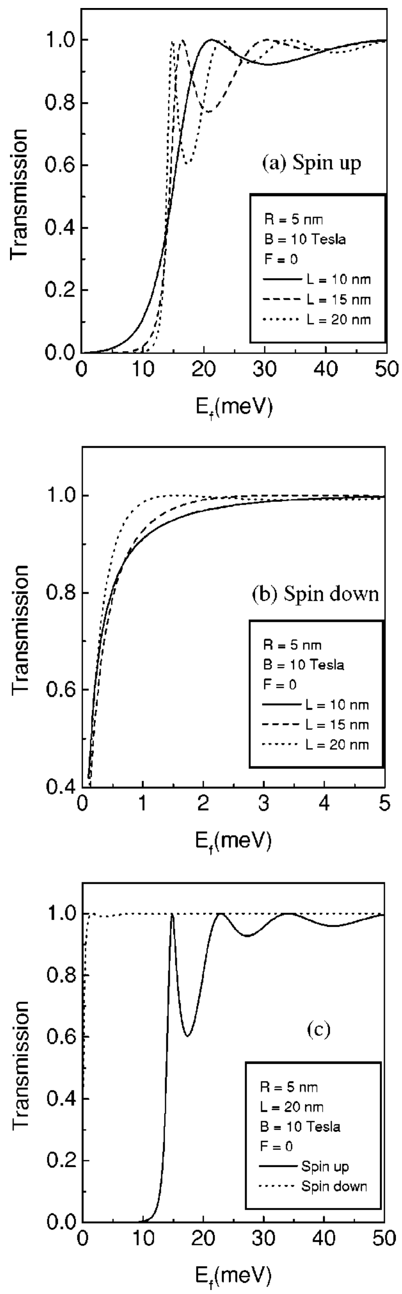

FIG. 1. The spin-dependent transmission coefficient as a function of the electron Fermi energy for the different system widths in $Cd_{0.93}Mn_{0.07}Te/Cd_{0.938}Mg_{0.062}Te$ system.

$$t^i = \Psi(z_N) = \prod_{p=0}^{N} S(z_p)\Psi(z_0). \tag{14}$$

The spin-dependent transmission coefficients of the system can be calculated by

$$T = \sum_i t^i. \tag{15}$$

The transmission coefficient in the above formula is dependent on the wave vectors k_x and k_y. For sufficiently large L_x and L_y it will be sufficient to use only $k_x = k_y = 0$.[5]

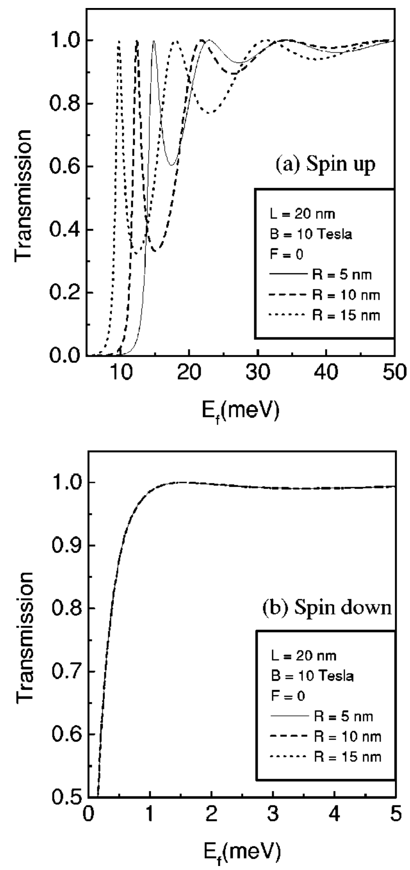

FIG. 2. The spin-dependent transmission coefficient as a function of the electron Fermi energy for the different QD radii in $Cd_{0.93}Mn_{0.07}Te/Cd_{0.938}Mg_{0.062}Te$ system.

III. RESULTS AND DISCUSSION

We consider an electron transport through a single $Cd_{1-x}Mn_xTe/Cd_{1-y}Mg_yTe$ spherical DMS QD. The spherical DMS QD is located at the middle of the system. The width of the system and the radius of the QD are $2L$ and R, respectively. The parameter used in our calculations are $x = 0.07$ and $E_c = 0.8(E_g^2 - E_g^1)$, where $E_g^1 = (1.586 + 1.51x)$ eV and $E_g^2 = (1.586 + 1.705y)$ eV are the band gap of $Cd_{1-x}Mn_xTe$ and $Cd_{1-y}Mg_yTe$, resepectively. $m^* = 0.096 m_0$,[7] where m_0 is the free-electron mass. $x_{eff} = 0.045$, $g\mathrm{Mn} = 2$, $N_0\alpha = 0.22$ eV, $N_0\beta = -0.88$ eV, $S_0 = 1.32$, $T_0 = 3.1K$, $g_e^* = -0.7$.[8]

A. The electron transport through a single $Cd_{0.93}Mn_{0.07}Te/Cd_{0.938}Mg_{0.062}Te$ spherical DMS QD system

In this section, we mainly consider the effect of spin split in a DMS QD. We set $E_c = 0$ for the $Cd_{0.93}Mn_{0.07}Te/Cd_{0.938}Mg_{0.062}Te$ system.[9]

Figure 1 shows the spin-dependent transmission coefficient as a function of the electron Fermi energy for different system widths. The radius of the QD is taken to be 5 nm. The magnetic field $B = 10$ T. Electric field $E = 0$. Figures 1(a) and 1(b) show the results for spin-up and spin-down electrons, respectively. The solid, dotted, and dashed lines are for $L = 10, 15, 20$ nm, respectively. Figure 1(a) shows that the

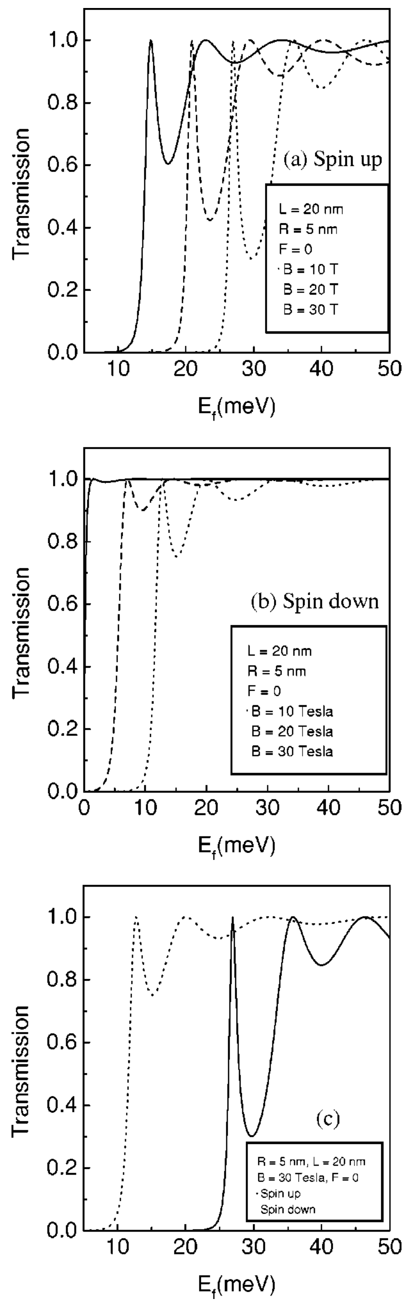

FIG. 3. The spin-dependent transmission coefficient as a function of external applied magnetic field in $Cd_{0.93}Mn_{0.07}Te/Cd_{0.938}Mg_{0.062}Te$ system.

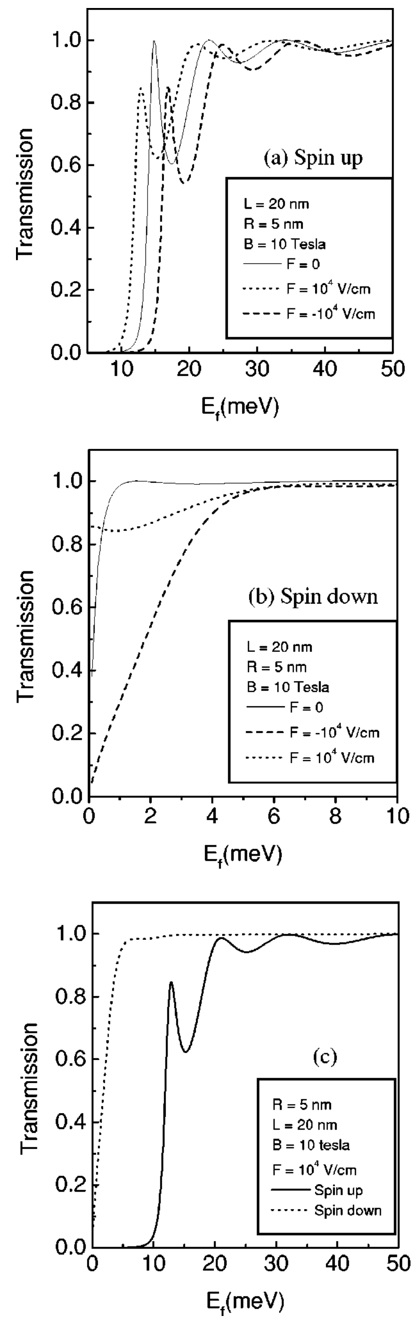

FIG. 4. The effects of an external static electric field on the transmission coefficient in $Cd_{0.93}Mn_{0.07}Te/Cd_{0.938}Mg_{0.062}Te$ system.

transmission coefficient increases quickly from near 0 to close to 1 at electron Fermi energy near 10 meV. The wider the system is, the more quickly the transmission coefficient increases. For spin-up electrons, the transmission is almost restrained if the Fermi energy is lower than 10 meV. Figure 1(b) shows that the transmission coefficient of the spin-down electrons almost equals 1 as long as the Fermi energy is greater than 1 meV. So, we can get a 100% polarized electric current by injecting electrons with 1–10-meV Fermi energy with the structure parameters given above. This characteristic can be clearly seen in Fig. 1(c).

Figure 2 shows the spin-dependent transmission coefficient as a function of the electron Fermi energy for different QD radii. The width of the system is taken to be 20 nm. The magnetic field $B=10$ T. Electric field $E=0$. Figs. 2(a) and 2(b) show the results for spin-up and spin-down electrons, respectively. The solid, dotted, and dashed lines are for $R=5$, 10, 15 nm, respectively. From Fig. 2(a) we find that the transmission peaks of spin-up electrons move to low Fermi energy side with increasing QD radius for a fixed system length. The reason is that the resonance energy levels along z direction will decrease for a larger QD and a fixed system length. For the spin-down electrons, the transmission is that of quantum wells, and the transmission is affected slightly by the QD radius.

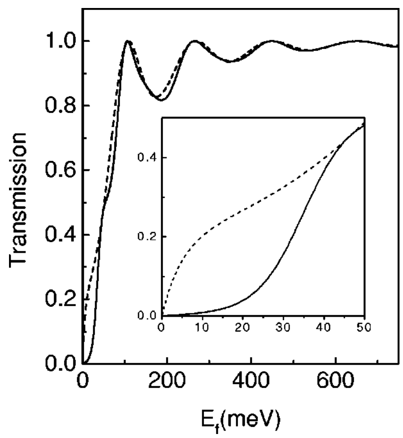

FIG. 5. The spin-dependent transmission coefficient as a function of the electron Fermi energy in $Cd_{0.93}Mn_{0.07}Te/Cd_{0.6}Mg_{0.4}Te$ DMS QD system. Solid and dashed lines correspond to spin-up and spin-down electrons, respectively. The structure and field parameters are $L=20$ nm, $R=10$ nm, $B=10$ T, $F=0$.

Taking into consideration the magnetic-field effects, we have calculated the spin-dependent transmission coefficient as a function of externally applied magnetic field. The results are shown in Fig. 3. The solid, dashed, and dotted lines correspond to the magnetic field $B=10$, 20, and 30 T, respectively. Let the radius of the QD be $R=5$ nm, the length of the system $L=20$ nm, and the external electric field $E=0$. The axial magnetic field along the z direction increases the transverse confined energy levels making the resonance peaks move to the high Fermi energy side for both the spin-up and spin-down electrons. This can be found in Figs. 3(a) and 3(b). Comparing Figs. 1(c) and 3(c), we find that the main difference between the spin-up and spin-down electron transmission is slightly enhanced for larger magnetic fields.

Figure 4 shows the effects of an external static electric field on the transmission coefficients, in which (a) and (b) are for spin-up and spin-down electrons, respectively. The solid, dotted, and dashed lines are for $E=0,10^4$, and -10^4 V/cm, respectively. The radius of the QD is $R=5$ nm, and the length of the system $L=20$ nm, the external magnetic field $B=10$ T. The external static electric field can move the transmission peaks to higher or lower Fermi energy side, depending on the direction of the external electric field. From Fig. 3(c) we find that the polarized electric current can also be present in an external static electric field.

B. The electron transport through a single $Cd_{0.93}Mn_{0.07}Te/Cd_{0.6}Mg_{0.4}Te$ spherical DMS QD system

In this section, we consider the effect of band offset. We have $E_c=461$ meV for the $Cd_{0.93}Mn_{0.07}Te/Cd_{0.6}Mg_{0.4}Te$ system.

Figure 5 shows the variation of the spin-dependent transmission coefficient with the electron Fermi energy for the $Cd_{0.93}Mn_{0.07}Te/Cd_{0.6}Mg_{0.4}Te$ DMS QD. The solid and dashed lines correspond to the results for spin-up and spin-down electrons, respectively. The structure and electric-field parameters are $L=20$ nm, $R=10$ nm, $B=10$ T, and $F=0$. Comparing with Fig. 1(c), we find that the difference between the spin-up and spin-down transmissions decreases as E_c increases. The reason is that the split energy between the spin-up and spin-down electrons can be treated as a perturbation, compared with large E_c.

IV. SUMMARY

In this paper, we have studied the transmission through $Cd_{1-x}Mn_xTe$ DMS QD's using the recursion method. The spin-dependent transmission can be tuned not only by the structure parameters but also by the external magnetic and electric fields. We can get a 100% polarized electric current by using suitable structure and external field parameters. Our calculated results may be useful for the application of $Cd_{1-x}Mn_xTe$ DMS QD's to the spin-dependent microelectronic and optoelectronic devices.

ACKNOWLEDGMENTS

This work was supported by the National Natural Science Foundation of China and the special funds for Major State Basic Research Project No. G2001CB309500 of China.

[1] S.A. Wolf, D.D. Awschalom, R.A. Buhrman, J.M. Daughton, S. von Molnar, M.L. Roukes, A.Y. Chtchelkanova, and D.M. Treger, Science **294**, 1488 (2001).

[2] Y. Guo, B.L. Gu, H. Wang, and Y. Kawazoe, Phys. Rev. B **63**, 214415 (2001).

[3] K. Chang and J.B. Xia, J. Phys.: Condens. Matter **14**, 13 661 (2002).

[4] Ph. Lambin and J.P. Vigneron, J. Phys. A **13**, 1815 (1981); J.P. Vigneron and Ph. Lambin, *ibid.* **13**, 1135 (1980).

[5] M. Brandbyge, K.W. Jacobsen, and J.K. Norskov, Phys. Rev. B **55**, 2637 (1997).

[6] B.V. Numerov, Mon. Not. R. Astron. Soc. **84**, 592 (1924).

[7] *Numerical Data and Functional Relationships in Science and Technology*, Landolt-Börnstein, New Series, Group X, edited by O. Madelung, M. Schulz, and H. Weiss, Vol. 17, Pt. a (Springer, Berlin, 1982).

[8] A.A. Maksimov, G. Bacher, A. MacDonald, V.D. Kulakovskii, A. Forchel, C.R. Becker, G. Landwehr, and L.W. Molenkamp, Phys. Rev. B **62**, R7767 (2000).

[9] J.A. Gai, R.R. Galazka, and Nawrocki, Solid State Commun. **25**, 193 (1978); Superlattices Microstruct. **16**, 5 (1994).